

A comparison of physical and numerical modeling of homogenous isotropic propeller blades *

Luca Savio^{1,2}, Lucia Sileo¹, Sigmund Kyrre Ås^{1,2}

¹SINTEF Ocean, Trondheim, Norway

²Norwegian University of Science and Technology (NTNU), Trondheim, Norway

ABSTRACT

Results of the fluid-structure co-simulations that were carried out as part of the FleksProp project are presented. The FleksProp project aims to establish better design procedures that take into account the hydroelastic behavior of marine propellers and thrusters. Part of the project is devoted to establishing good validation cases for fluid-structure interaction (FSI) simulations. More specifically this paper describes the comparison of the numerical computations carried out on three propeller designs that were produced in both a metal and resin variant. The metal version could practically be considered rigid in model scale, while the resin variant would show measurable deformations. Both variants were then tested in open water condition at SINTEF Ocean's towing tank. The tests were carried out at different propeller rotational speed, advance coefficients and pitch settings. The computations were carried out using the commercial software STAR-CCM+ and Abaqus. The paper describes briefly the experimental setup and focuses on the numerical setup and the discussion of the results. The simulations agreed well with the experiments, hence the computational approach has been validated.

Keywords

Fluid structure interaction, Propulsion

1 INTRODUCTION

The topic of hydroelastic behavior of marine propellers is nowadays often associated with the behavior of composite propellers that aim at using some sort of anisotropy to achieve some set goal. The goal may be reducing vibrations or cavitation. In the past Atkinson and Glover [1] have shown numerically how full-scale metallic propellers could bend under the action of hydrodynamic forces to an extent that, for some particular propeller geometries, namely blades with large skew angles, could have some significance in terms of propeller performance. The numerical method adopted was a combination of lifting line and finite element methods (FEM) in what we would call a weak co-simulation, in modern terms. Nowadays co-simulations are increasingly carried out coupling CFD (Computational Fluid Dynamics) with FEM (Finite Element Method) code. The coupling between the two

codes vary from weak to strong, according to how the two simulations communicate in terms of time increments and variables that are transferred. While this has been a research area for quite some time, modern software implementations have reached a level of maturity that makes these types of analysis attractive also at the level of industrial design engineers. The increased ease of setting up co-simulations should not however be taken as a guarantee for obtaining accurate results. In fact, the accuracy of the computations should be verified and compared with results obtained in controlled scenarios, as, for example, during open water tests in a towing tank or cavitation tunnel. The validation of numerical results by means of experiments presents a series of challenges that require careful preparation and interpretation of the results. It is important to limit the scope of what can be validated by means of experiments; it is practically impossible to designing experiments that allow for correctly scaling to laboratories size displacements and forces of some full scale hydroelastic phenomenon. What is possible is to design experiments that allow for their correct representation in the simulation codes with the aim of validating the latter. In this paper we present the results from experiments carried out on three propeller designs that have been produced with blades both in aluminum and in a casting resin resembling an epoxy resin, hence presenting a rigid and flexible behavior, respectively. The three propellers share the same design parameters apart from the skew distribution. The tests have been performed in a classical open water configuration at different propeller speeds and at different pitch settings. The open-water configuration was chosen so that the hydroelastic behavior was limited to static deflection, i.e. vibrations of the blades were avoided by performing the tests in a homogenous inflow.

2 MODEL PRODUCTION

2.1 Propeller geometries

Three propeller geometries were generated starting from a master geometry varying the skew distribution. The master geometry is labeled P1374 and was designed using SINTEF Ocean proprietary propeller design code AKPD [2]-[3]. Propeller P1374 has a balanced skew distribution that amounts to 23 degrees.

The first variation, P1565, was obtained by removing entirely any skew distribution. In the second variation, P1566, the same total skew as propeller P1374 was kept, but in an unbalanced form. The geometries of the blades are not reported here because of space limitations, but they can be obtained upon request since the FleksProp consortium decided to allow disclosing the propeller geometries.

2.2 Production of flexible blades

The flexible blades were manufactured using resin casting under vacuum, which is a commonly used technique in rapid prototyping. In order for resin casting to be used, it is necessary to produce a positive object that is then used to make a silicon mold where the resin is cast under vacuum and left to cure. Three complete controllable pitch propellers, including the hubs, were produced in aluminum according to the production standard used in SINTEF Ocean. One blade per kind was then sent to a company specializing in rapid prototyping, PROTOTAL AS, that produced 5 copies of the blade.

According to the producer of the resin used for casting, the Young's modulus is equal to 2.2 GPa. The Poisson's ratio is not reported, but given the nature of the material, it was assumed to be equal to 0.33. The material properties reported by the producer have not been checked by mechanical testing; however, the good agreement between computations and experiments indicates that the reported values can be considered accurate.

3 MODEL TESTS

The model tests have been carried in the SINTEF Ocean large towing tank between the month of February and June 2018. The setup adopted was the classical open water configuration where the propeller is placed in front of the dynamometer. The dynamometer used in the test was a Kempf & Remmers H29 model. Figure 1 shows that only the surfaces in contact with water located on the left side of the 1mm gap contribute to the forces measured by the dynamometer.

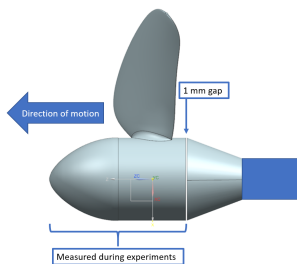


Figure 1: Experimental setup showing which surfaces contribute to the forces measured during the experiments

According to standard procedures for open-water tests, a dummy hub without blades was tested to obtain forces on the cap and hub at different velocities. The forces measured during the test with the dummy are then subtracted from the forces measured with the actual propeller, to obtain what is traditionally referred to open water curves. The traditional way of presenting the data tries to isolate the blades from the propeller. When the experimental data is to be compared with CFD results, it is more consistent to use the uncorrected (raw) force measured during the experiments, and compute the forces on the above mentioned surface on the measuring side of the gap.

The open-water tests were performed at 3 different propeller rotational speeds, 7, 9 and 11 rps in the range of advance coefficients from 0 to 1.2 in 0.2 steps for the pitch setting $P/D = 1.1$ and from 0 to 1.05 in 0.15 steps for the pitch setting 0.9. Tests were also performed at $P/D = 1.2$, but the results from this pitch setting have not been simulated yet.

The experimental relative uncertainty at 95% confidence for the thrust and torque coefficients has been evaluated using the methodology described in [7], and found to be weakly dependent on the advance coefficient J as Figure 2 shows for P1374 at $n = 7$ rps. Slightly smaller values of the uncertainty were found for the other rps. The uncertainty reported here is relative only to propeller P1374, but similar values were found also for the other propellers.

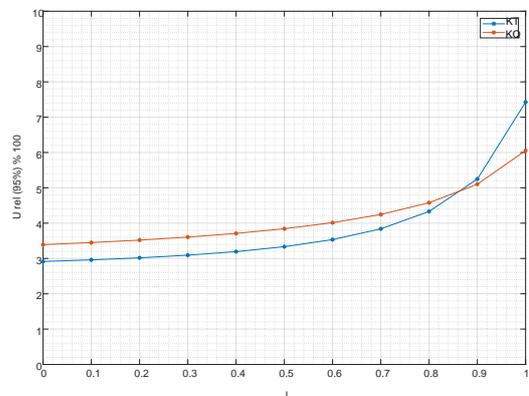


Figure 2: Example of relative uncertainty for propeller P1374 at P/D 1.1 and $n=7$

4 FSI SIMULATIONS

Fluid-structure interaction (FSI), generally speaking, is the thermo-mechanical interaction of one or more solid structures with an internal or surrounding fluid flow. FSI problems play prominent roles in many scientific and engineering fields, such as mechanical, aerospace, and biomedical engineering. Thanks to the recent advances of commercial software, numerical simulations have become a feasible and valuable way to investigate the fundamental physics involved

in the complex interaction between fluids and solids. Nevertheless, there is still the need for validation when these tools are used in new applications.

When using a numerical procedure, an FSI problem is usually described in terms of a fluid domain and a structural domain, and in-between there is a fluid-structure interface. This multi-physics problem with adjacent domains can be simulated in a monolithic or in a partitioned way [6]: the former simultaneously solves the governing equations for fluid and structure within a unified algorithm, and it requires a code developed for this particular combination of physical problems. In contrast, the partitioned approach treats the fluid and the structure as two computational fields which can be solved separately with their respective mesh discretizations and numerical algorithms, and the boundary conditions at the interface are used explicitly to relay information between the fluid and structure solutions. This enables the use of existing well-established fluid and structural solvers, which represents a significant motivation for adopting this approach. In addition to the fact that, for many problems, the staggered approach works well, is very efficient and preserves software modularity. Difficulties may arise however, in terms of robustness and accuracy, for specific problems, like for example flutters or parachute problems [5]-[4].

In the present case, we consider the problem of viscous incompressible fluid flow interacting with an elastic body (the propeller blade) immersed in the flow, and being deformed by the fluid action. A staggered approach is used, coupling two different solvers that uses different methods and codes: a CFD/FVM solver (Computational Fluid Dynamics/Finite Volume Method) for fluids and FEA/FEM (Finite Element Analysis/Method) for structure mechanics.

In ‘two ways’-FSI, the results of the CFD solver, in terms of hydrodynamic forces on the interface, are mapped from the fluid model to the structural model and provided to the structural equation solver; the results obtained by the structural solver are mapped back to the first model, in terms of displacements of the interfacial surface, involving the modification/morphing of the mesh of the fluid model. The procedure is repeated until convergence. How often this mapping needs to be performed depends on the degrees of coupling, and it is related to the response times of the structure compared to the fluid: in case of strong coupling, the mapping may be needed in the internal time-step iterations, inside each time step, following an implicit method.

In the present case, the fluid and structure are ‘weakly’ coupled, because the response of the structure to a disturbance in the fluid is slow compared to the fluid. As seen from the experiments, a ‘static’ solution is expected, which means that one can search for a steady-state condition, corresponding to the shape the structure takes in the stationary fluid when reached the

hydro-elastic equilibrium, corresponding to the steady-state flow around the deformed blade. All these considerations have important consequences on the flexible-blade simulations:

- explicit algorithm can be used, which means that the fluid and the structure solvers are not necessarily in the processor memory at the same time and that the mapping between the two codes may happen at each time-step (and not at each internal iteration)
- the analysis does not need to be time accurate, as an equilibrium state with a static solution is desired
- material damping can be increased
- first-order integration in time may be used

4.1 Numerical setup

In the present work, STAR-CCM+ v12.04, by Siemens PLM Software, is used as CFD code and Abaqus 2016, by Dassault Systèmes, as FEM code. An open-water simulation was used as a starting point, with the following characteristics: the computational domain is corresponding to one-blade passage only, the MRF (Multi-Reference Frame) approach is used, which means that the propeller rotation is not simulated with the actual rotation of the mesh but it is modeled using a reference system rotating with the blades and solving the equations of motion in this reference system, once the boundary conditions have been correctly set up on the propeller surfaces with the proper value of velocity.

The computational domain and boundary conditions are illustrated in Figures 3 and 4. It is a 90° sector of a cylinder, whose axis corresponds to the propeller axis of rotation and radius equal to 10 propeller diameters. The propeller is located in the region highlighted in red in Figure 4 where a polyhedral mesh is generated, and then extruded further upstream and downstream, toward the inlet and outlet boundary respectively.

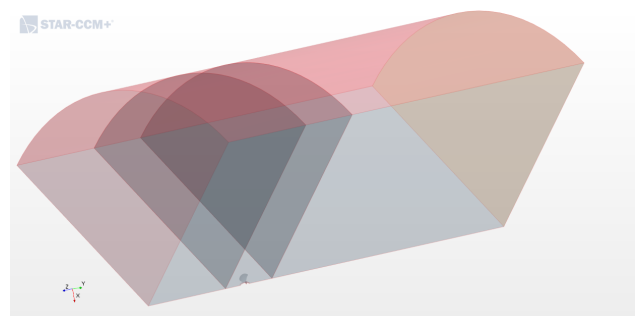


Figure 3: Computational domain.

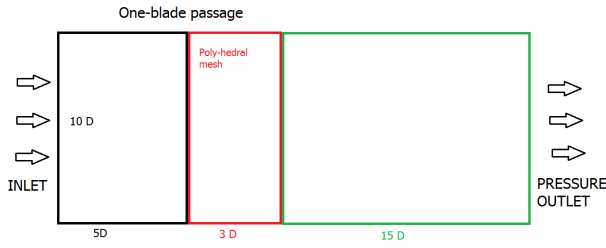


Figure 4: Domain size and boundary conditions.

The geometry of the numerical propeller model is kept as close as possible to the one used in the experiments, including the gap of 1 mm between the hub and the cone; the housing is modeled with infinite length, extended up to the outlet.

A longitudinal section of the volume mesh is depicted in Figure 5. The mesh, for all the considered cases, consists of about 1.6 M cells, including 10 layers of prismatic layers at the wall. The thickness of the first prismatic layer is set to approximately have Y^+ of the order of 1 on the blades. The Gamma-ReTheta transition model is used for turbulence, which performed better than the SST-K- ω and the RST model; the reason is because at model scale there are likely areas of the blades subjected to laminar flow with transition to turbulent flow.

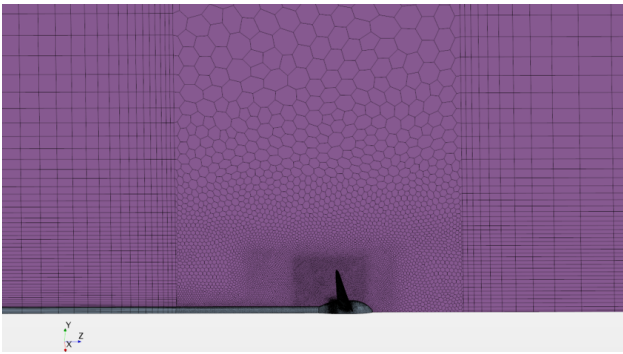


Figure 5: Longitudinal section of the volume mesh.

The structural mesh consisted of $2.1 \cdot 10^5$ tetrahedral elements and was generated by the Abaqus mesher. To determine the mesh number of cells, a mesh refinement study was performed where the mesh was refined until the displacements at the blade tip were no longer changing. Figure 6 shows an example of a structural mesh.

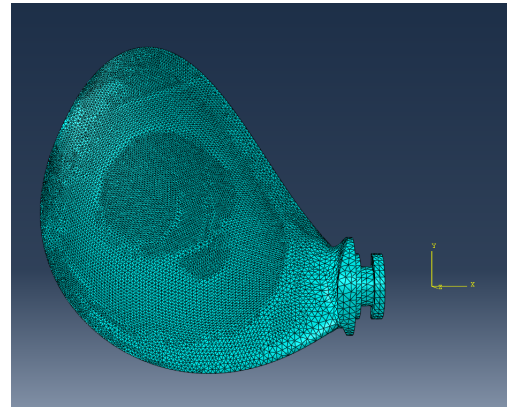


Figure 6: Example of structural mesh

For the structural part of the computations, it is important to model the root of the blade and the fastening system. The blade root is built in the same resin as the rest of the blade and has several contact surfaces that constrain it to the propeller hub. The different contact surfaces determine different boundary conditions. In Figure 7 the different boundary conditions are identified with different colors; the red surfaces are encastre type boundary condition, while the green surface identifies a surface that allows only rotation along the direction perpendicular to the surface and translations in the plane identified by the surface.

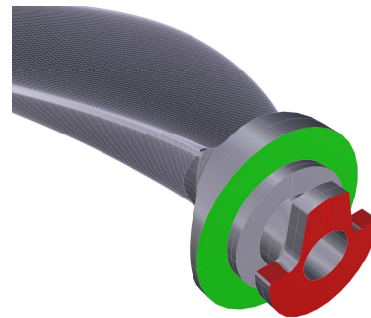


Figure 7: Boundary condition at the blade root

The three propellers designs, P1374, P1566 and P1565, are analyzed. Initially the open-water calculations are carried out for the rigid case, with reference to the model tests with the aluminium propellers. The resulting flow field is then used as initial flow state for the CFD-FEM co-simulations, activating the Abaqus and the morpher solvers.

The mapping is managed by StarCCM+, where the co-simulation set-up is accomplished by identifying the coupled model parts, the exported/imported fields (pressure/displacements) and specifying the external code execution details (commands, input files, etc.).

4.2 Results

A converged solution of the co-simulation is reached well before the simulation time, initially fixed to 10 s,

with time step of 0.005 s , as shown in Figure 9, where the axial displacements at different locations of the blade are monitored during the simulation, for the propeller P1374, $P/D = 1.1$ and $n = 11\text{ rps}$. The results obtained for the three propellers at $P/D = 1.1$ and $P/D = 0.9$ are reported in Figure 14 and 15 respectively: k_T , k_Q , η obtained by the co-simulation are plotted as a function of the advance ratio J both for the aluminum propeller and for the (flexible) resin propeller, and compared to the experimental values. The agreement is very satisfactory, also in terms of the relative increase of the coefficients in the flexible case with respect to the rigid one. Except for the bollard condition and for the $J = 1$ case, where the blades can experience flow with ‘negative’ angle of attack and subsequent separation and unsteadiness, the difference between the numerical results and the experimental data is less than 2% in terms of thrust coefficients, as shown for example in Figure 8, where the differences for k_T , k_Q and η_0 are shown for the propeller P1374, $P/D = 1.1$.

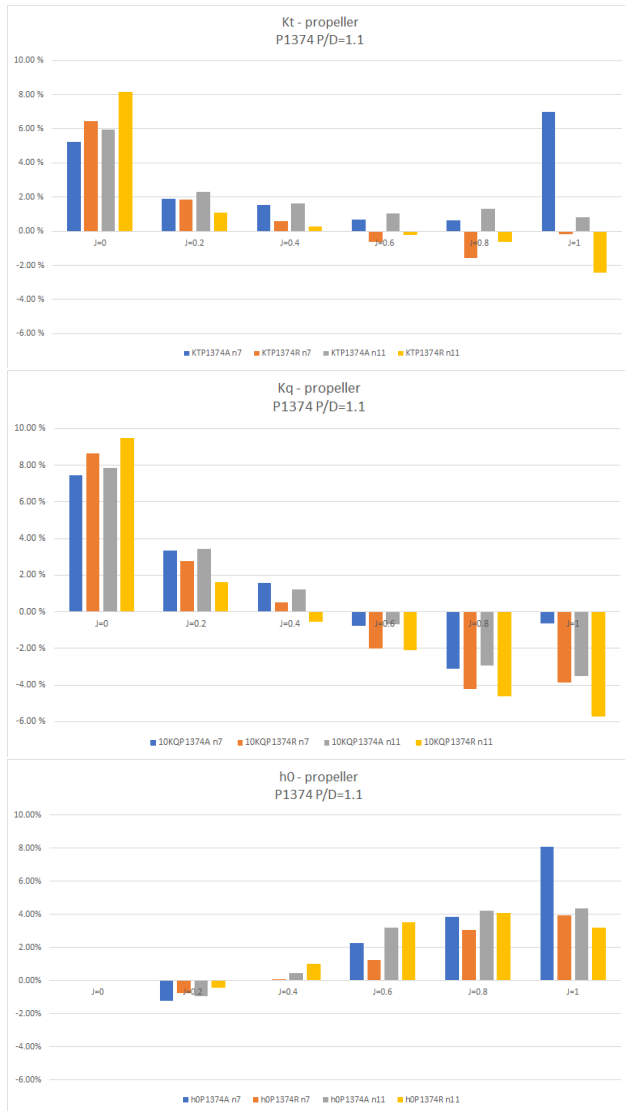


Figure 8: Propeller P1374, $P/D = 1.1$, $n = 7$ and $n = 11\text{ rps}$: relative differences between numerical and experimental data, in terms of thrust and torque coefficients and propeller efficiency.

Note that, with reference to Figure 2, the deviation seen between CFD and experiments is, in most cases, within the uncertainty bands of the experiments.

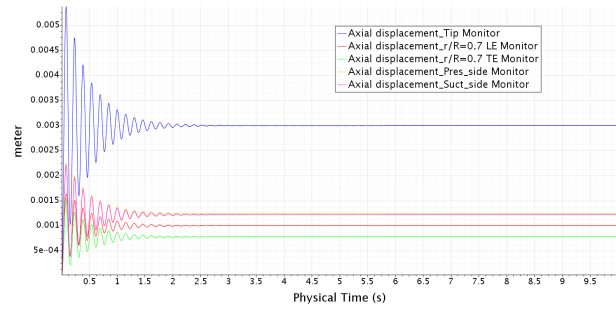


Figure 9: Propeller P1374, $P/D = 1.1$ $n = 11\text{ rps}$: axial displacements at different locations of the blade monitored during the simulation.

4.3 Blade displacements

It is rather straightforward to extract the blade cylindrical section displacements from the numerical computations, and compare the effect of the different skew distributions of the three blades. One way, that seems quite natural, is to decompose the displacements of the sections in terms of bending and twisting. In this approximation the bend is defined as the average displacement of the blade sections in the YZ plane, where Z is the propeller advance direction, X the radial direction and Y the direction perpendicular to both X and Z . Twist is defined as the rotation of the blade section in the same YZ plane. Some results for this twist definition are shown in Figure 10 and Figure 11. Close to the tip, the twist component is correctly identified, while erroneous results appear closer to the blade root. Still, this presentation will be used here since it offers a compact way of presenting the data. Note also that the reservations on the bend-twist presentation of the data apply only to twist. It was expected that the elastic behavior of the low aspect ratio propeller blades could only partially be represented by pure bend and twist of the blade sections. It is important to keep in mind this finding when trying to implement design codes that are based on lower order theories, as for example lifting line theory coupled with beam theory. Even with the reservation that have just been described, it is possible to use the bend-twist approximation to explain the effect of the propeller skew on propeller blades that are otherwise identical. In Figure 12 and 13 the bend and twist of the sections from the radial location 0.4 to 0.975 are plotted.

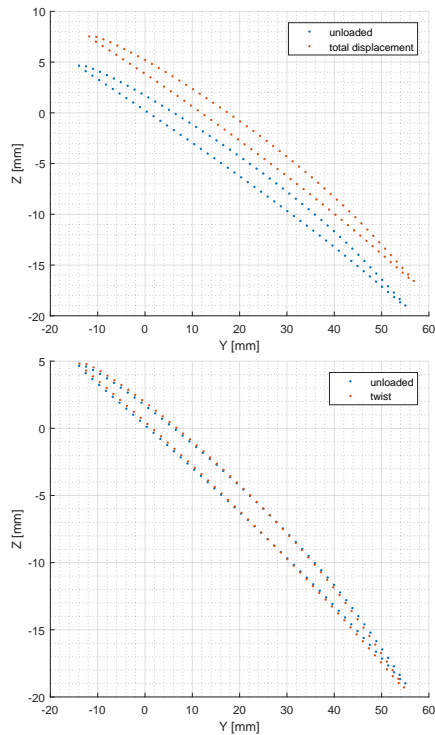


Figure 10: Bend and twist of a typical blade section towards the tip

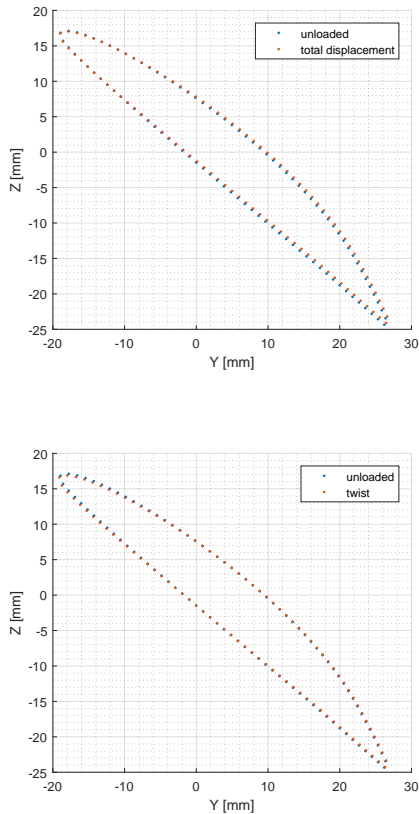


Figure 11: Total displacement and twist of a section close to the blade root

As expected, the different skew distributions of the three geometries have limited effect on the propeller bending, while the effect is clearly seen on the blade twist. The skew distribution influences the relative position of the pressure center and the elastic center, and this can result in a bend-twist coupling also for homogeneous - isotropic materials. The balanced skew distribution, a very common choice among propeller designs, featured by P1374 is the one that shows the least twisting of the three different blade designs. Although it is in principle possible to use the skew distribution for controlling, possibly only to a small degree, the bend-twist coupling of propeller blades, the skew distribution is decided based on considerations regarding the wake distribution and its effect on cavitation of the blades.

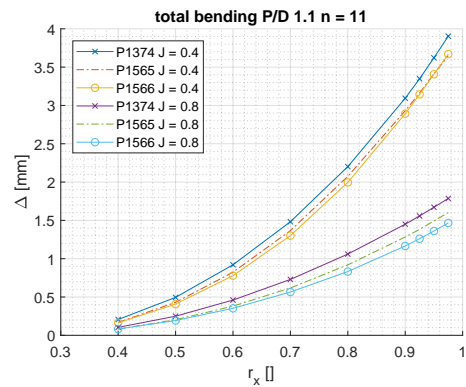


Figure 12: Bending of the three different blade geometries at $P/D = 1.1$ and 11 rps

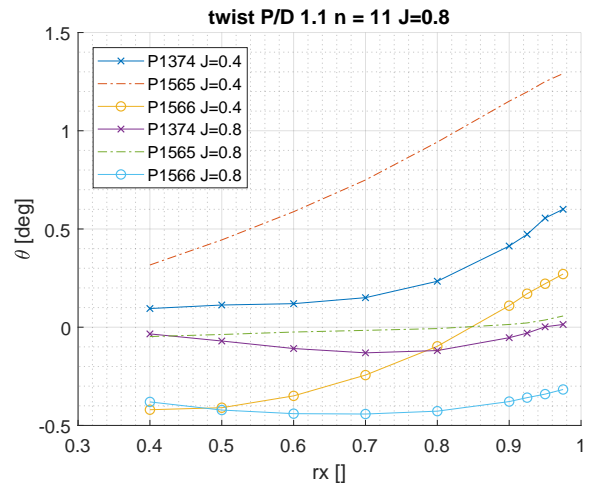


Figure 13: Twist of the three different blade geometries at $P/D = 1.1$ and 11 rps

CONCLUSIONS

In this paper the validation of Fluid Structure Interaction computations for flexible propeller blades, carried out using the co-simulation approach, has been described. The validation data comes from a series of ad-hoc tests performed with the specific aim of serving as a reference for numerical computations. For the experiments, three propellers

were manufactured both in a metallic and plastic material in order to have rigid and flexible models. The propeller geometries and the experimental data are public domain, and can be obtained upon request. The simulated values of thrust and torque coefficients lie mostly within the bands of experimental uncertainty, showing how CFD-FEM co-simulations can be used to accurately represent the behavior of homogeneous isotropic blades tested in open water. Furthermore, the thrust coefficients seem to compare better than the torque coefficients. It is often reported that in model scale CFD simulation, the torque coefficient suffers from deviation that are larger than those observed on the thrust coefficient, a phenomenon that is often attributed to the laminar to turbulent transition of the flow on the model scale blades. Since the Reynolds numbers of full-scale propellers are higher, it is to be expected that CFD can better predict the full-scale torque coefficient, since the flow is mainly turbulent, a fact that makes the approach described here even more valuable.

ACKNOWLEDGMENTS

The present work has been fully supported by the FleksProp project. The FleksProp project is cooperation between SINTEF Ocean, the Norwegian University of Science and Technology NTNU and Rolls Royce Marine with the economic support of the Research Council of Norway (RCN) and Rolls Royce Marine. The economic support of the Research Council of Norway and Rolls Royce Marine is greatly appreciated.

REFERENCES

- [1] Atkinson, P. & Glover, E.J. (1988). 'Propeller hydroelastic effects'. Propellers 88 Symposium, Virginia Beach, Virginia, September 20-21, 1988.
- [2] Achkinadze, A.S., Krasilnikov, V.I. (1999). 'A Numerical Lifting-Surface Technique for Account of Radial Velocity Component in Screw Propeller Design Problem. Proceedings of the 7th International Conference on Numerical Ship Hydrodynamic NSH7, July 19-22, Nantes, France.
- [3] Achkinadze, A.S., Krasilnikov, V.I. and Stepanov, I.E. (2000). 'A Hydrodynamic Design Procedure for Multi-Stage Blade-Row Propulsors Using Generalized Linear Model of the Vortex Wake. Proceedings of the Propellers/Shafting'2000 SNAME Symposium, Virginia Beach, VA, September 20-21.
- [4] Bazilevs, Y., et al. (2008). 'Isogeometric fluid-structure interaction: theory, algorithms, and computations'. Computational Mechanics, 43:3-37, 2008.
- [5] Degroote, J, et al.(2010). 'Performance of partitioned procedures in fluid-structure interaction'. Computers & Structures, Vol. 88, Issues 7-8, pp. 446-457, 2010.
- [6] Hou, G., Wang, J., Layton, A. (2012). 'Numerical Methods for Fluid-Structure Interaction - A Review'. Communications in Computational Physics, Vol. 12, Issue 2, pp. 337-377, 2012.
- [7] JCGM 100:2008 GUM 1995 with minor corrections - valuation of measurement data — Guide to the expression of uncertainty in measurement
- [8] Savio, L.(2015): Measurements of the deflection of a flexible propeller blade by means of stereo imaging. SMP2015 - The Fourth International Symposium on Marine Propulsors; 2015-05-31 - 2015-06-04
- [9] Yin L. Young, Nitin Garg, Paul A. Brandner, Bryce W. Pearce, Daniel Butler, David Clarke, Andrew W. Phillips, Load-dependent bend-twist coupling effects on the steady-state hydroelastic response of composite hydrofoils, Composite Structures, Volume 189, 2018, Pages 398-418, ISSN 0263-8223, <https://doi.org/10.1016/j.compstruct.2017.09.112>.

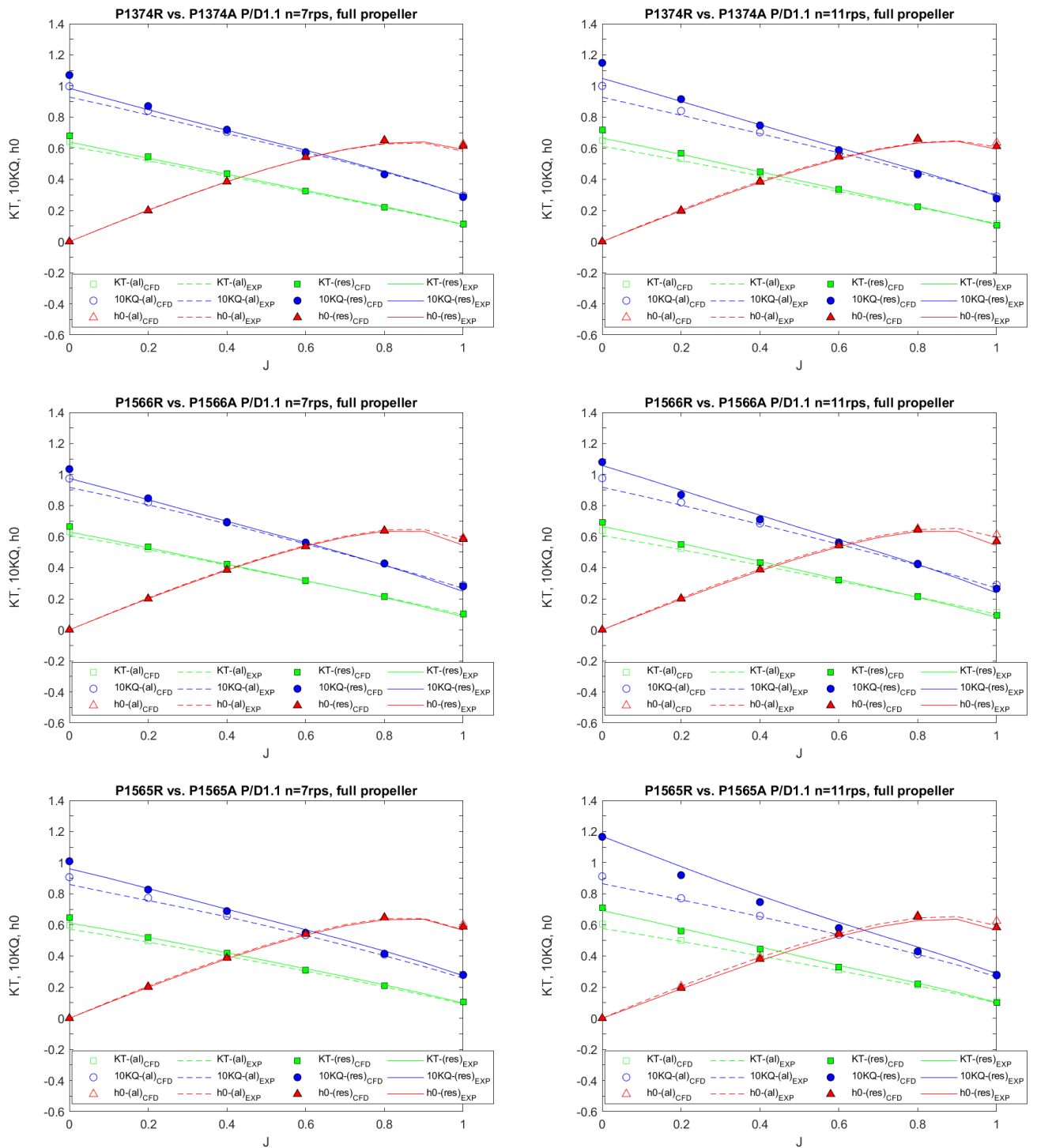


Figure 14: Results $P/D = 1.1$

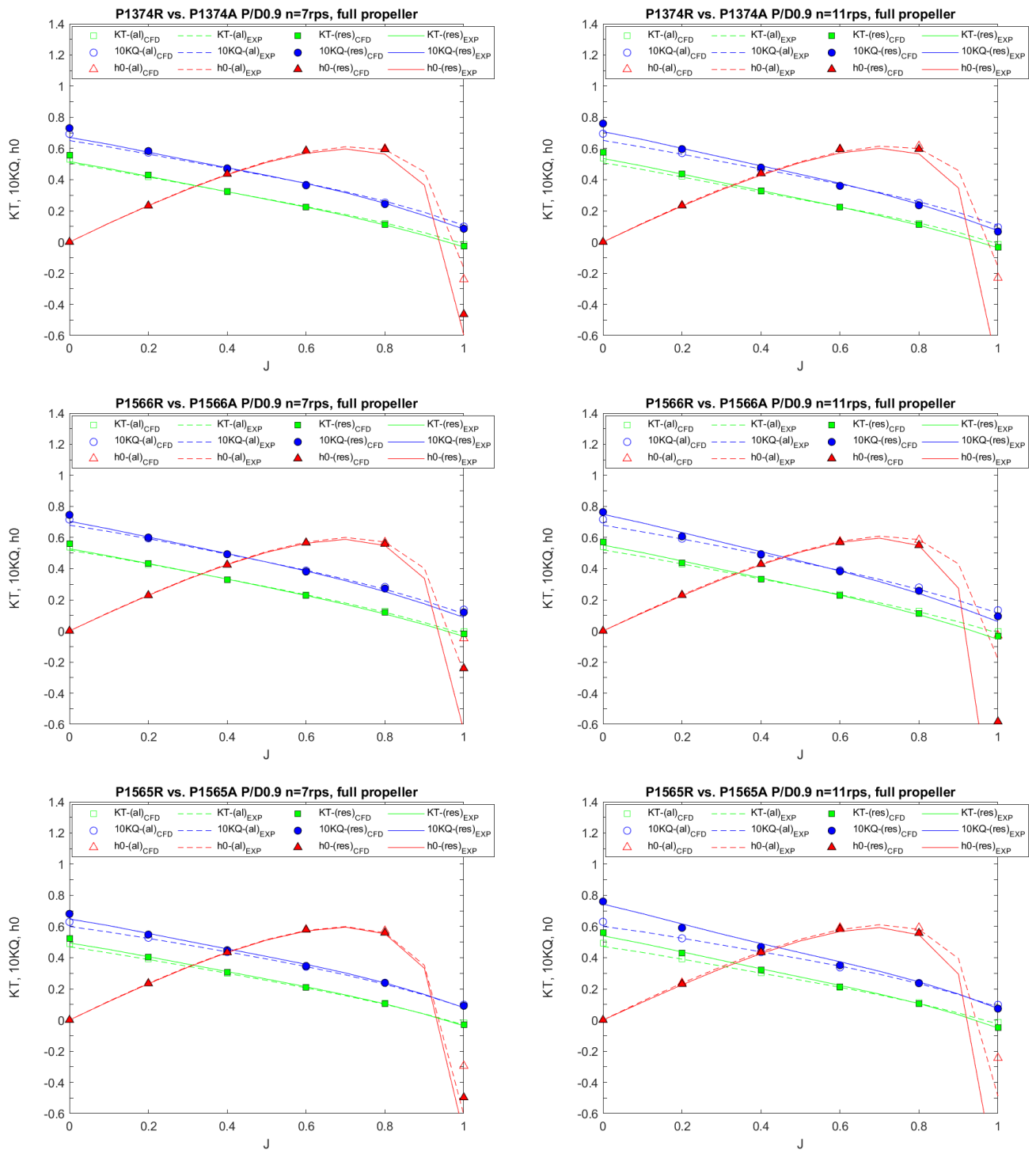


Figure 15: Results $P/D = 0.9$